AD-A170 158 ACTA ARMAMENTARII (SELECTED ARTICLES)(U) FOREIGN 1/1
TECHNOLOGY DIV WRIGHT-PATTERSON AFB OH 08 JUL 86
FTD-ID(RS)T-0069-86

UNCLASSIFIED F/G 19/1 NL

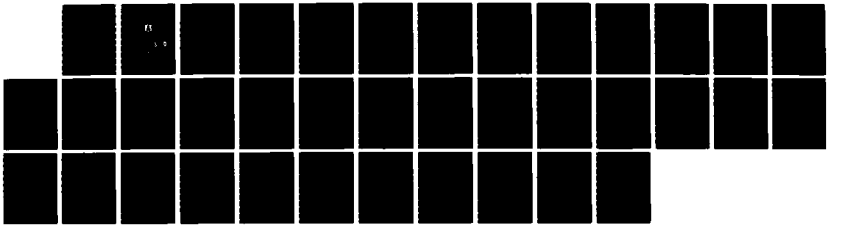

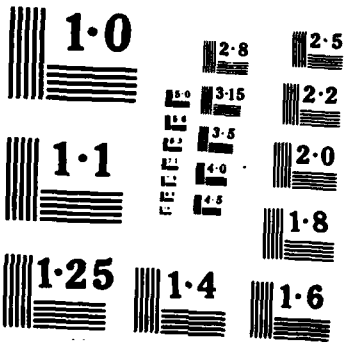
1·0
1·1
1·25
1·4
1·6
1·8
2·0
2·2
2·5
2·8
3·15
3·5
4·0
4·5

(2)

FTD-ID(RS)T-0069-86

FOREIGN TECHNOLOGY DIVISION

AD-A170 158

ACTA ARMAMENTARII

(Selected Articles)

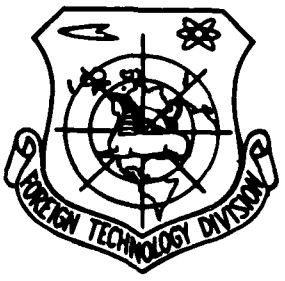

Approved for public release;
Distribution unlimited.

HUMAN TRANSLATION

FTD-ID(RS)T-0069-86 8 July 1986

MICROFICHE NR: FTD-86-C-001997

ACTA ARMAMENTARII (Selected Articles)

English pages: 32

Source: Binggong Xuebao, Nr. 2, May 1985, pp. 26-31; 49-58

Country of origin: China
Translated by: SCITRAN
F33657-84-D-0165
Requester: FTD/TQTR

PREPARED BY:

TRANSLATION DIVISION
FOREIGN TECHNOLOGY DIVISION
WPAFB, OHIO.

Table of Contents

GRAPHICS DISCLAIMER

All figures, graphics, tables, equations, etc. merged into this translation were extracted from the best quality copy available.

THE SYSTEM OF TIMELY MEASUREMENT OF BURN RATES OF SOLID PROPELLANTS BY LINE SCAN

MA QUNGYUN, SUN PEIMAO, LIU DALI, LI YUPING

Abstract

Owing to the emerging of microcomputer and the application of line scan camera, it is possible for us to link up these two modern instruments and to apply them to measure the burn rate and combustion process of solid propellants. This is a new rapid photo-electric method. In this paper, the instantaneous optical image of combustion process of A and B two propellants is transformed to numerical signals by CCD line scan camera. Then the signals enter a PS-80 microcomputer and stored in its memories. We can obtain the figure of pellet length versus time by plotter. The average burn rate and pressure exponent and various tables of data by printer. All data can be stored in tapes.

1. INTRODUCTION

In the past several years, designers of various weapons require solid propellants with high or super high burn rates. But, conventional measuring techniques, (the trajectory technique, the photographic technique)have certain limitations. For instance, measuring the burn rate with the trajectory technique can only tell the average burn rate over a length of 100 or 50 mm. It is not able to clarify the burning process, or the burning mechanism. Determining the burn rate of solid propellants with the high speed photographic

technique is not suited because of the effects of the brightness of the light source, the sensitivity of the film, the aperture, the temperature and the time of developing and fixing. Furthermore, the test period is too long and costs too much money.

To measure the burn rate of solid propellants, the photographic technique (1) is superior to the trajectory technique, but it can only obtain a picture of the burning process and can not convert the picture into numbers. The scientific method must analyze the burn parameters by numbers.

One can investigate the burn rate and burning process of solid propellants with a solid camera CCD (Charge Coupled Device) and a microcomputer. This is a new rapid photo-electric method (2) (3). It has the following advantages:

1) It is able to show tiny changes in the burning process of solid propellants, dynamite, and gun-powder, and then to determine the burning stability of sample columns.

2) The precision is high; it is able to precisely measure a propellant with a burn rate as high as 1000 mm/s. The relative error is 0.44%; particularly for propellants with high burn rates, its precision is better than conventional methods.

3) It is capable of converting optical signals into electric signals. This can be combined with a microcomputer to analyze the numbers automatically, thus increasing the test speed.

4) The dose of tested sample for a single test is only 1.5g. The method is safe and economical, and favourable for developing new

versions.

2. EXPERIMENTAL EQUIPMENT AND TECHNIQUES

This system used a PS-80 microcomputer for analyzing data. The main computer CPU was a Z-80 with 48 KB, the CCD input signals were input through a DI/DO connector. A printer and a chart recorder were used for data output.

The software was designed with a top to bottom method, and multistage subprograms were built in. The program was written in BASIC and in compilation language. The whole program was divided into 7 blocks. To satisfy the multistage data collecting and the experimental result analysis, the data collecting was transferred in compilation language for high-speed requirements.

Three blocks and seven different functions were used in data processing and data output, according to the controling, printing, displaying, listing and chart recording, reporting formats. The input of the original data and the operation of the program were performed in a system of five cycle communication. Thus the whole experimental system had great flexibility.

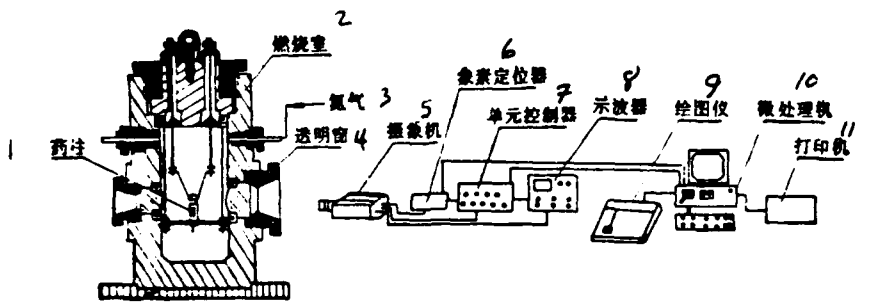

Fig. 2.1 The schematic diagram of the system for measuring the burn

rate

1. Sample column 2. Combustor 3. Nitrogen 4. Transparent window 5. Camera 6. Image element fixer 7. Control unit 8. Oscilloscope 9. Chart recorder 10. Microcomputer 11. Printer

The expansibility and the stability of this software were very good. For data with large capacities only some subprograms had to be added to match the disk system.

The photoelectric transfer system consists of a charge coupled device camera with 1024 image elements, a control unit, an image element fixer, and a microcomputer matching circuit. After a sample column, 7mm in diameter and 20 mm in length, was lit, the burned part was illuminated by the burning flame, the boundary between the burned and unburned parts, and the brightness distribution of the flame area formed an image on the CCD through an optical lens. The exposure time and data rate were determined by the control unit. The CCD was exposed, spot by spot, from top to bottom. This produced an electric signal immediately. After the image element fixer determined the position of the signal jump line (i.e. the boundary between the burned and unburned parts), the computer could then collect the data under the control of the matching circuit.

The collected address codes of image elements were transfered into the corresponding lengths by the PS-80 computer. Then, the curves of the sample length 1 versus the burning time t were plotted on an X-Y chart recorder. The numbers could be either printed out or stored. The instantaneous burn rate, the average burn rate, and the

pressure parameter of the burning process were also calculated.

The results of measuring the burn rate of A-type solid propellant at a pressure of 10^4 kPa are shown in Table 2.1, Figures 2.2 and 2.3. The results for a B-type propellant are shown in Figures 2.4 and 2.5. The relationships between the burn rate and the pressure of A-type and B-type solid propellants are shown in Fig. 2.6.

Fig. 2.2 shows that after 0.6 seconds after being lit the A-type sample column started burning steadily. Its 1-t curve is in a wave-like form; this can be seen more clearly in Fig. 2.3.

The average burn rate u_{ave} and the instantaneous burn rate can be calculated from the collected data in Table 2.1.

The calculation formula of the average burn rate is:

$$u_{ave} : \frac{l_2 - l_1}{t_2 - t_1}$$

where l_1, l_2---lengths of sample columns

t_1, t_2---corresponding burning time of l_1, l_2.

Table 2.1 Relationship between the sample length and burning time for A-type solid propellant at 10^4 kPa.

l /mm	t /ms	l /mm	t /ms
0.686191	30.887517	6.31576	31.612987
0.154043	33.965274	12.2814	37.966365
3.12287	40.340633	0.630176	42.692924
7.35205	46.694011	1.8065	49.068283
0.57416	53.069370	1.0783	57.070457
0.0420117	59.444728	1.47041	63.445816
1.19033	67.446899	1.47041	71.447998
0.182051	75.449081	0.630176	79.472152
1.63846	83.473236	1.63846	87.474327
1.8065	91.475418	0.378105	95.476501
0.910254	99.499572	1.8065	103.50066
1.83451	107.50175	2.08658	111.50283
0.462129	115.50392	1.19033	119.50501
1.97455	123.52808	1.89053	127.52917
2.39467	131.53025	0.798222	135.53135
1.35838	139.53242	2.19861	143.55551
2.03057	147.55659	2.5067	151.55767
1.10631	155.55877	1.66646	159.58183
2.36666	163.58293	2.19861	167.58401
2.84279	171.58509	1.41439	175.58619
⋮	⋮	⋮	⋮
12.4775	1553.4772	12.4775	1557.4782
12.5335	1561.4793	12.8416	1565.5025
12.8416	1569.5035	12.5335	1573.5046
12.7856	1577.5057	12.9536	1581.5068
13.0936	1585.5299	13.0096	1589.5310
12.9536	1593.5319	12.8696	1597.5332
13.0096	1601.5343	13.3177	1605.5572
13.2337	1609.5583	13.1497	1613.5595
13.0936	1617.5605	13.2897	1621.5616
13.5698	1625.5847	13.5138	1629.5858
13.4017	1633.5869	13.2897	1637.5880
13.4017	1641.5891	13.6818	1645.6121
13.7378	1649.6132	13.6818	1653.6143
13.6818	1657.6153	13.7378	1661.6165
13.9059	1665.6395	13.8499	1669.6406
13.7378	1673.6417	13.7378	1677.6429
13.9059	1681.6439	14.214	1685.6669
14.1579	1689.6680	14.0179	1693.6691
13.9619	1697.6702	14.1299	1701.6713

Using only two points to calculate the average burn rate is not as accurate as calculating the average value using all data between these two points, collected by the computer.

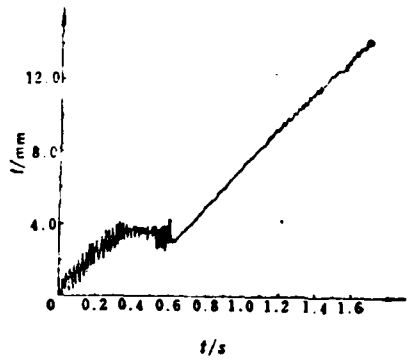

Fig. 2.2 The 1-t curve of A-type solid propellant at 10^4 kPa.

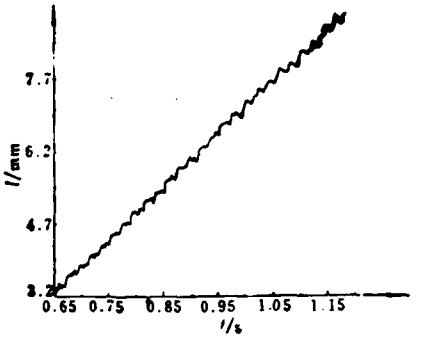

Fig. 2.3 The enlargement of a part of the curve in Fig. 2.2 (t from 0.65 ~ 1.15s).

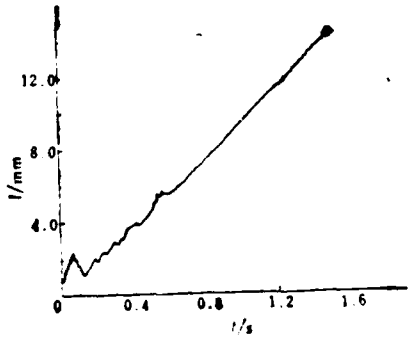

Fig. 2.4 the 1-t curve of B-type solid propellant at 10^4 kPa.

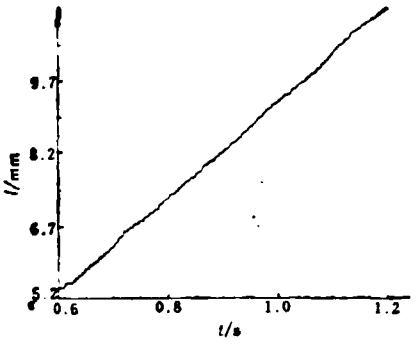

Fig. 2.5 The enlargement of a part of the curve in Fig. 2.4 (t from 0.6 ~ 1.2s).

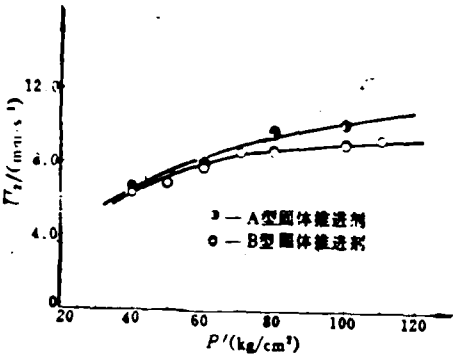

Fig. 2.6 The relationships between burn rate and pressure of A-type and B-type solid propellants.

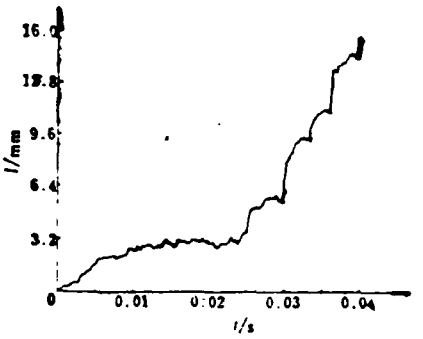

Fig. 2.7 The l-t curve of porous composite gunpowder (4×10^3 kPa).

3. DISCUSSION OF THE EXPERIMENTAL RESULTS

As shown in Fig. 2.2, when A-type solid propellant started burning, probably because of the lighting with a heating wire, the external heat was substantial. It burned unsteadily. The flame was irregular and fluctuated. But, 0.6 seconds later, burning was continued by the heat produced by the A-type solid propellant itself. Therefore, the burning became steady at a steady rate.

Although the A-type solid propellant was burning with a steady rate, as apparently shown in Fig. 2.2, its burning surface was fluctuating up and down significantly (about 0.4 mm). This was probably caused by the thin liquid layer formed on the surface of the A-type solid propellant. That layer was boiling during the burning process. To prove this proposed explanation, we stopped the burning process of an A-type sample, and observed a solidified liquid layer on its burned surface.

Experiments using a line scan camera and a microcomputer to investigate the instant burn rate, the average burn rate, and the burning process of the A-type solid propellant showed that this is a good method. The burn rate of any short interval in the burning process can be calculated from Fig. 2.2. This enabled us to easily know the burning state at any instant. If the burn rate changed, the position of the change point can be determined. This is very helpful in understanding the reason for unsteady burning. Therefore, this is superior to measuring the average macroscopic burn rate between two points, 50 mm or 100 mm apart, with the trajectory technique.

When measuring burn rates of solid propellants with this system, for a sample with a burn rate of 100 mm/s, we were able to obtain 30 instant burn rates for every mm of the sample. For a sample with a burn rate of 1000 mm/s, we were able to obtain 3 instant burn rates for every mm of the sample. According to these data, we were able to explore the detailed change in the burning process easily.

The burning pattern of B-type solid propellant was different from the A-type one. The latter's burning surface fluctuated substantiallly (about 0.4 mm). The former's burning surface fluctuated less (about 0.08 mm), and the burning process was more steady.

As shown in Fig. 2.4, the B-type solid propellant started burning steadily 0.6 s after being lit. Its burn rate at 10^4 kPa was 9.4 mm/s.

Using a microcomputer, we are able to collect a great deal of burning information data through CCD. For instance, for the sample

length listed in Fig. 2.1 (13 mm), 418 data points were obtained (adjusting equipment can speed up data collecting). Then, the burning pressure parameter could be calculated automatically through the program. Because of the large number of collected data points, the calculation results are accurate. These are capable of showing the real burning process. Therefore, it is easier for designers of rockets, missiles, and spacecraft to design the engines.

The 1-t relation of special porous high burn rate composite gunpowder, obtained by using this system is shown in Fig. 2.7. It took only 0.04 s for a sample with 1=16.1 mm to burn out. Its average burn rate u_{ave}=400.2 mm/s. As shown in the same figure, there were two burning rates in two stages of its burning process. From the beginning to 1=3.2 mm, its burn rate was 133.3 mm/s, but from 1=3.2 mm on, its burn rate increased tremendously, and the burn rate was 806.2 mm/s. It can thus be seen that its burn rate increased by a factor of 6. 1=3.2 mm was the turning point of the burn rate.

A large number of experiments were performed for testing the accuracy of this system. One of them was using this system to measure a specified micrometer. The relative difference between the displays of the micrometer and this system was 0.2%.

Moreover, the burn rates of 8 samples of A-type solid propellant were measured with this system under same pressure, same original temperature, same density of the sample, and same sample length. The relative difference was 0.44%.

4. CONCLUSION

(1) The line scan camera system is capable of investigating the burn rate and the burning process of solid propellants. Its accuracy is high, and it is capable of calculating any instantaneous burn rate at any time.

(2) Using a microcomputer to measure the burn rate of solid propellants, all the collected data and the calculated results can ba displayed, printed out, plotted, and stored. Also, its average burn rate and burning pressure parameter can be calculated.

(3) This method uses very little sample dose (each sample is 1.5g) and obtains very accurate data, thus makes experiments safe and economical. Because the dose of an experimental sample is so small, it is easy to make samples, thus perform experiments move faster, and shorten the period of developing new products.

(4) Experiments showed that CCD transferred photoelectric signals quite well. It was capable of transferring the burning information of solid propellants to a microcomputer in real time.

(5) Experiments showed that the matching circuit between the microcomputer and CCD worked quite well.

(6) Experiments showed that using a microcomputer to collect the burning information through a DI/DO connector is quite successful.

(7) This system is capable of investigating the burn rate and burning process of solid propellants with high burn rates. Experimental results showed that the burn rate of the porous

composite gunpowder in the high burn rate region was 806.2 mm/s.

All of the above confirm that this measuring system is one of the new modern techniques of investigating the burn rate and burning process of solid propellants.

References

[1] A.П. 格拉兹圆娃著，马庆云译，《爆炸物燃烧的催化作用》，北京，国防工业出版社，1982年。

[2] 岩间 彬等，"采用光电晶体管测定固体火箭推进剂燃速"，《工业化学杂志》1962,65,№8，P.1218～1219，(日文)。

STUDIES ON THE DYNAMIC MECHANICAL PROPERTIES OF THE COMPOSITE MODIFIED DOUBLE-BASE PROPELLANT

Zhou Zhou Jia Zhanning and Zhou Qihuai

Abstract

The dynamic mechanical properties of the composite modified double-base (CMDB), double-base (DB) and polyvinyl chloride(PVC) composite propellants were measured respectively with a Rheovibron viscoelastometer. The effects of three kinds of solid fillers [aluminium (AI), ammonium perchlorate (AP) and cyclotetraethylenetetranitramine (HMX)] and the different kinds and contents of plasticizers [triacetin (TA), ortho-dibutyl phthalate (DBP) and nitroglycerine (NG)] on the dynamic mechanical properties of the double-base binder were studied. The dynamic mechanical data and spectrums on these ingredients have been obtained at a fixed frequency (3Hz) and a broad range of temperature. At the same time, the impact strengths of the CMDB propellant, the double base binder and the pvc propellant were also measured at a broad range of temperature. Experimental conclusions have been obtained that the dynamical mechanical properties of the CMDB propellant lie between the DB and PVC composite propellants and depend on its binder system and that the CMDB propellant has the specific properties of both higher mechanical damping and a strong β relaxation at low temperature.

As reported in the literature, since the early sixties the United States has been using various dynamic measuring equipment to measure and study the dynamic mechanical properties of solid propellants (1). Recently, England started working on the same problem (2). They were mainly interested in composite propellants (e.g. U.S.). So far, no reports on studying the dynamic mechanical properties of CMDB propellant have been published. Domestically, there were attempts to measure the dynamic mechanical properties of solid propellants with a twisting technique and a spring vibrating technique.

Investigating the dynamic mechanical properties of CMDB propellant with a Rheovibron viscoelastometer and studying the effect of component concentration on its mechanical properties are reported in this paper.

1. Experimental Samples and Experimental Techniques

1.1 Experimental Samples

The specific formula for each experimental sample is listed in Tables 1.1-1.3

1.2 Experimental technique

1.2.1 Dynamic Experimental Technique

The phase difference between sine stress and sine strain, so-called dissipasion angle S, and the absolute value of the complex modulus [E] of samples under dynamic stretching were measured with a ZNP Rheovibron viscoelastometer over a wide temperature and wide fixed

frequency range. Moreover, from these following formulas one can obtain:

The energy storage modulus $E' = [E^*] \cos \delta$ N/m^2

The dissipation modulus $E'' = [E^*] \sin \delta$ N/m^2

The dissipation factor $tg\delta = E''/E'$

Table 1.1 Experimental sample formulas (1)

5 含量 / 组分 6 / 4 样品序号	NC	NG	7 安定剂	黏结剂与8 工艺附加物	Al	AP	HMX
1#	65.50 / 1	32.80 / 0.5	1.70 / 0.026				
2#	49.35 / 1	49.35 / 1	1.30 / 0.026				
3#	40.43 / 1	58.51 / 1.45	1.06 / 0.026				
4#	33.04 / 1	66.09 / 2	0.87 / 0.026				
5#	36.20 / 1	52.40 / 1.45	0.95 / 0.026	10.45 / 0.29			
6#	26.57 / 1	38.46 / 1.45	0.70 / 0.026	7.70 / 0.29	26.57 / 1		
7#	30.16 / 1	43.65 / 1.45	0.79 / 0.026	8.73 / 0.29		16.67 / 0.55	
8#	19.00 / 1	27.50 / 1.45	0.50 / 0.026	5.50 / 0.29	Al + AP + HMX = 47.5%		
9#	24.59 / 1	35.59 / 1.45	0.65 / 0.026	7.12 / 0.29	32.05 / 1.3		
10#	24.59 / 1	35.59 / 1.45	0.65 / 0.026	7.12 / 0.29		32.05 / 1.3	
11#	24.59 / 1	35.59 / 1.45	0.65 / 0.026	7.12 / 0.29			32.05 / 1.3

note:

(1) sizes of the used solid grains: Al 8.7 μm

AP 86 μm

HMX 92 μm

(2) the concentration in this table:

shown as the weight concentration %/the ratio of the composite concentration

/to the NC content

(3) samples in this table were all made by casting

(4) sample numbers

(5) concentration

(6) composite

(7) settling agent

(8) flux and manufacturing additive

Table 1.2 Experimental sample formulas (2)

1 含量/% 组分 3 / 样品序号	NC	NG	TA	DBP
12#	66.67		33.33	
13#	66.67			33.33
14#	66.67	33.33		

(1) sample number

(2) concentration/%

(3) composite

note: samples in this table were all made by calendering

Table 1.3 Experimental sample formulas (3)

DB Propellant		PVC Propellant	
composite	concentration/%	composite	concentration/%
NG	55	PVC	12.5
NG	29.3	AP	70
flux	10	plasticizer	17.0
settling agent	3.0	stabilizer	0.5
trajectory improver	0.9	burn rate regulator	0.05
additive	1.8		(additional)

Note: (1) NC: nitroglycerine

(2) PVC propellant was manufactured by casting

(3) DB propellant was manufactured by extruding in spirals

The experimental conditions:

sample size: lenght x width x depth = 2~5 x 0.1~0.5 x 0.01~0.2 cm^3.

temperature increasing rate: 2°C/min

experimental temperature region: -10~°C~+160°C

experimental frequency: 3 Hz

1.2.2. Impact Method

The equipment used was a pendulum type impact detector. The experimental conditions were as follows:

potential energy of the pendulum: 10 kg.cm

width of the opening: 4.0 cm

impact speed: 2.87 m/s

sample size: 5.5 x 0.5 x 0.5 cm3 (samples had no flaws)

experimental temperature region: -100°C~+30°C

time for keeping samples in fixed temperatures: 30 min

impact strength a was calculated by the following formula

$$a = \frac{\text{the work needed to break the sample}}{\text{the cross-section of the sample}} \quad (kg.cm/cm2)$$

2. Experimental results

Table 2.1 Tg and T_β of each sample under 3 Hz dynamic condition

sample no.	1*	2*	3*	4*	5*	6*	7*	8*
T_g/°C	84.2	52.4	34.0	25.6	31.1	32.4	31.0	31.2
T_β °C	-29.5	-33.7	-41.1	-46.5	-36.6	-31.2	-36.8	-36.2
sample no.	9*	10*	11*	12*	13*	14*	DS	PVC
T_g/°C	21.8	33.7	32.3	59.8	52.1	1[illegible].2	65.1	-21.6
T_β °C	-35.1	-34.1	-37.7	10.8*	-30.7	-36.2*	-4.7	—

* obtained by drawing a tangent line

All graphs of experimental results are shown in tables 3.1 through 3.12. The glass transition temperature Tg and the β transition temperature T_β deduced from the temperature corresponding to the maximum of the dissipation factor tgδ for each sample are listed in table 2.1

3. Discussion

According to the regular dynamic analysis, the characteristic regions of the viscoelastic behaviour of tested materials were deduced from E'-t curves, their mechanical damping were investigated with tgδ-t curves. The experimental results are discussed as follows.

3.1 Dynamic Mechanical Properties of CMDB propellant

(1) As shown in Fig. 3.1 and Table 2.1, under 3 Hz dynamic condition, the

mechanical damping peaks of glass transition occured at different temperature regions for three propellants. For PVC propellant, Tg (=-21.6°C), much lower than room temperature, so it has already shown rubber-like properties at room temperature. For DB propellant, Tg (=65.1°C),(much higher than room temperature) it is thus a plastic material at room temperature. For CMDB propellant, Tg(=31.2°C) (at the vicinity of room temperature) it does not show the mechanical behaviour of typical plastic or typical rubber-like materials at room temperature. Practically, it mainly shows transition properties.

(2) As shown in Fig. 3.1, DB and CMDB propellants show a significant second transition (β transition or β relaxation) when the temperature is below Tg, while PVC propellant does not show this.

When the temperature is between -50°C ~ +70°C (regular temperature region for propellants to be used), CMDB propellant has the highest mechanical damping peak, and has a significant β relaxation dissipation at lower temperature. For the entire temperature region, CMDB propellant has larger mechanical damping.

Reference [3] claimed that CMDB propellant was applicable for temperature and vibrating conditions at sea, and used it as the propellant of the auxiliary engine for the ship missile "Ocean Javelin." This showed that they took good advantage of the high mechanical damping of this propellant.

(3) As shown in Fig. 3.2, when temperature is between -100°C and +100°C, E' of CMDB propellant is between that of DB and PVC propellants. In the temperature region of propellants (-50°C∿+70°C), CMDB propellant goes through the glass phase region (-50°C∿+6°C), the glass transition region (6°C∿50°C), and the high elastic phase region (50°C∿70°C). Because it underwent the second transition at -60°C, its glass had already relaxed, E' had been decreasing all along. Compared to the glass phase with a fixed modulus, it has certain deformation capability in the low usage temperature range. On the other hand, the transition region determined by the modulus decrement is so wide that it almost covers most usage of the temperature range (-50°C∿+50°C). Therefore, in the usage temperature region it has very strong mechanical damping property. In the usage temperature range, DB propellant goes through the glass phase region (-50°C∿+40°C) and the glass transition region (40°C∿70°C). Because of its high Tg, it stays in the glass phase usage for most of the temperature range. Although its glass phase also undergoes the β relaxation, E' is still very high

and decreases slowly, thus the deformation hardly occurs. For temperatures between -50°C~+70°C, PVC propellant is basically in the glass transition state and the high elastic phase; also its Tg is low, the modulus is small and decreases fast, so it is a kind of propellant with very good flexibility in the temperature range.

As shown in the analysis above, the differences in the dynamic mechanical properties among these three propellants are rather large. Besides the different formulas and composite concentrations, the main reason is that they have different structural origins (nitrocellulose for CMDB and DB propellants, polyvinyl chloride for PVC propellant). The main differences of propellants with the same origin are the different manufacturing method (CMDB is made by casting, DB is made by extruding in spirals) and the different cotton dissolution ratios (DB: NC/solvent =1.26, CMDB: NC/solvent=0.57), besides, CMDB contains many solid additives.

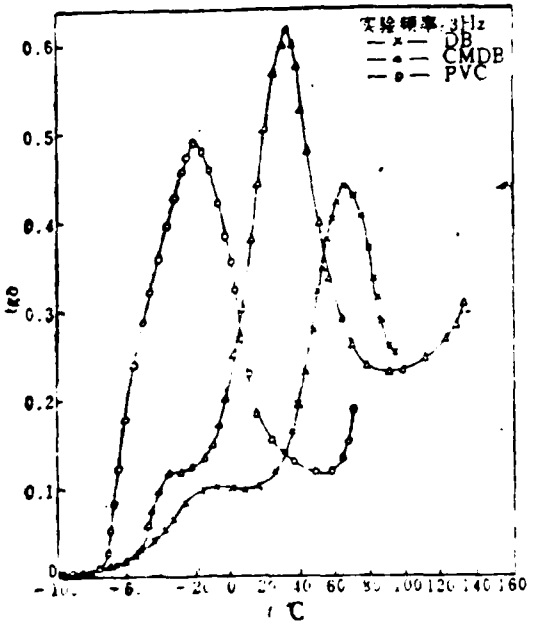

Fig.3.1 tgδ -t curves of DB, CMDB, and PVC propellants.

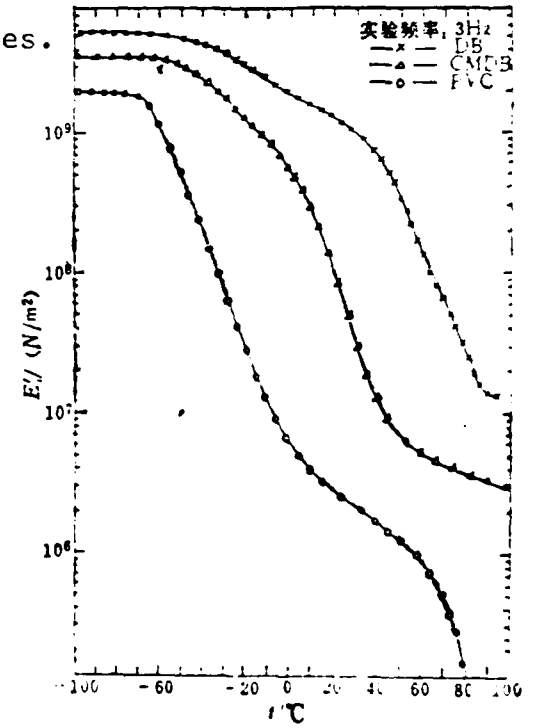

Fig. 3.2 E' -t curves of DB, CMDB and PVC propellants.

3.2 The relation between the dynamic mechanical properties and the antiimpact properties for CMDB propellant.

Presently, it has been proved (4-7) by experiments in several polymers that the significant β relaxation of a polymer enables it to increase its impact strength at temperatures below Tg. It is already known in our experiments that CMDB propellant has fairly strong β relaxation. Our impact experiments verified that it had higher impact strength in the glass phase.

As shown in Fig. 3.3, the impact strength of CMDB propellant has two increase points with the increasing temperature. This shows that its β relaxation can cause fairly big mechanical damping. Therefore, below the temperature, at which the motion of chain segments enhances the impact strength tremendously, it is able to dissipate a lot of impact energy, and to prevent or slow down creation and development of the cracking and thus enhance impact strength. It is known from observation and analysis of the cracking section that from -50°C to - 30°C, the surface of a cracking section changes from smooth to rough, from glossy to no gloss. It has a remarkable property of transition from fragile cracking to tenacity cracking. Therefore, under this impact condition, for CMDB propellant, at least at T above - 30°C, it is tenacity cracking.

Nielson (8) has pointed out that if E"/E' is lower than 0.02, hard polymers are usually fragile, with low impact strength; if the ratio is greater than 0.10, the material usually has high impact strength. As shown from data in this paper, the tg δ of CMDB propellant is greater than 0.02 when the temperature is above -52.6°C.

It is greater than 0.10 when the temperature is greater than -36.5°C. Thus it can be seen that for a 3 Hz dynamic condition, CMDB propellant has certain tenacity at T above -52.6°C, while at T higher than -36.5°C, it should have fairly high impact strength. As shown in Fig. 1, these deduced results all fall in the β relaxation region. Furthermore, -36.5°C, coincides with its T_β (=-36.2°C). Impact testing has already shown that the presence of the β relaxation is related to the impact strength. Therefore, CMDB propellant can be used at temperatures between Tg and T_β. Because the double-base binder also has β relaxation, results similar to CMDB propellant are obtained for it. PVC does not have β relaxation. When T becomes as high as the temperature of the main chain segment motion (-60°C), the impact strength just starts to increase rapidly. Compared to CMDB propellant, it can only be used at T above Tg which is its main chain segment motion temperature. It can thus be seen that for CMDB propellant, it is not proper to treat Tg as a low temperature limit for use. The effect of its strong β relaxation on its dynamic mechanical properties should be considered.

3.3 The effects of solid fillers on the dynamic mechanical properties of the double-base binder

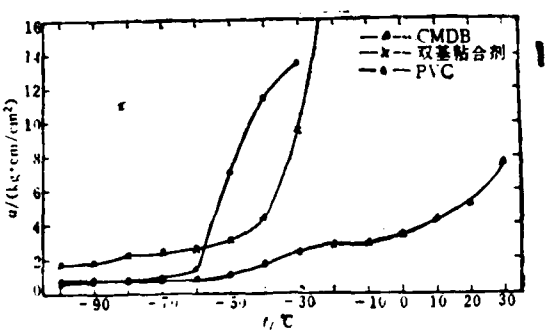

Fig. 3.3 Impact strength versus temperature. α-T for CMDB, binder and PVC.

1 - binder

The effects of solid fillers on the dynamic mechanical properties of the double-base binder are shown in Fig. 3.4, Fig. 3.5 and Fig. 3.6. As shown in

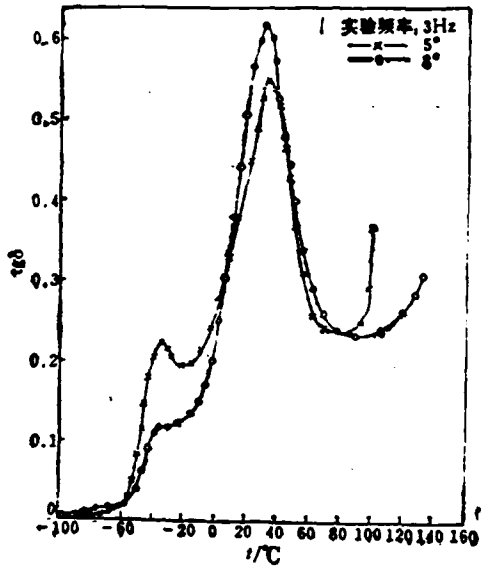

Fig. 3.4 tgδ-t curves of samples 5* and 8*.
1 - frequency

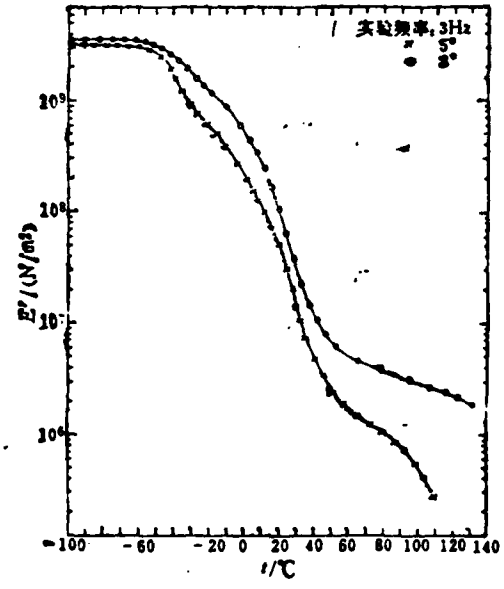

Fig. 3.5 E'-t curves of samples 5* and 8*.
1 - frequency

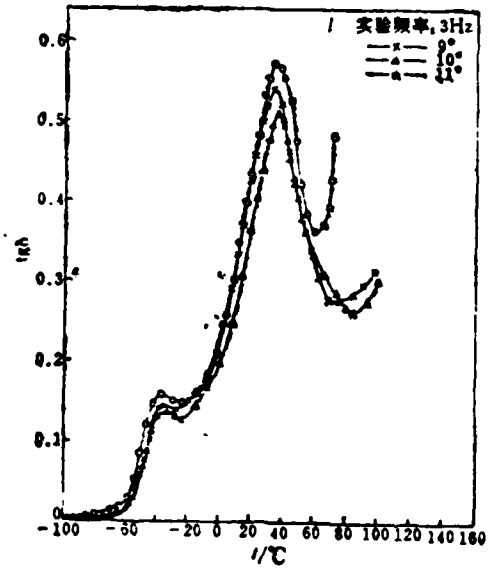

Fig. 3.6 tg δ -t curves of samples 9*, 10* and 11*.
1 - frequency

figures, tg_δ of the double-base binder sample (5*) and solid filler added samples (6*~11*) apparently increase in the vicinity of -60°C. They all have fairly strong β relaxation. The two peaks of mechanical damping for binder samples do not show apparent deviation after adding different fillers. Their transition temperatures are close to each other. But, adding these fillers apparently lowers the peak of β damping. Moreover, the effects of these three fillers on the mechanical damping of the double-base binder are the same. After these added samples undergo β relaxation (all about -60°C and above), the β relaxation is enhanced with increasing temperature, their E' is higher than E' of unadded samples, and is enhanced apparently in the high elastic region. This agrees with the dynamic mechanical behaviour of average polymers after rigid fillers are added. This agrees with the effects of solid fillers on the dynamic modulus of composite and nitro-plastic colloid propellants, described in other papers.

3.4 The effects of plasticizers on the dynamic mechanical properties of double-base binders.

(1) The effects of fluxes and manufacturing additives

Sample 3 is a sample of the double-base binder without fluxes and soluble manufacture additive. Compared to sample 5 (Table 2.1, Fig. 3.7), since there are very small amounts of flux and manufacturing additives in CMDB propellant, their effects on the dynamic mechanical properties and on two transition temperatures of the binder are not significant.

(2) The effects of different concentrations of nitroglycerine (NG) (Fig. 3.8, 3.9, 3.10)

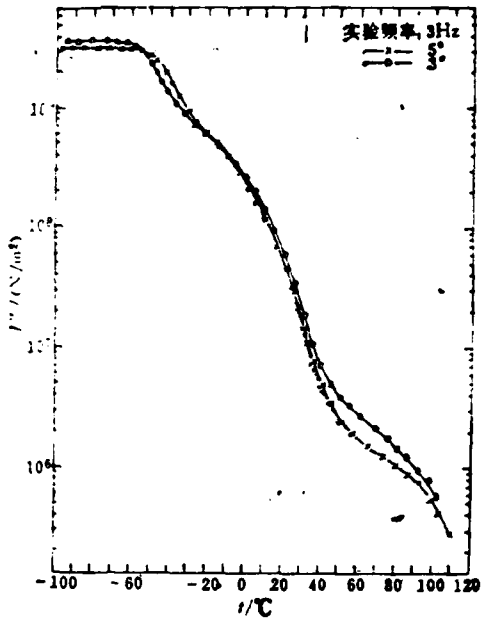

Fig 3.7 E' -t curves of samples 3* and 5*.
1 - frequency

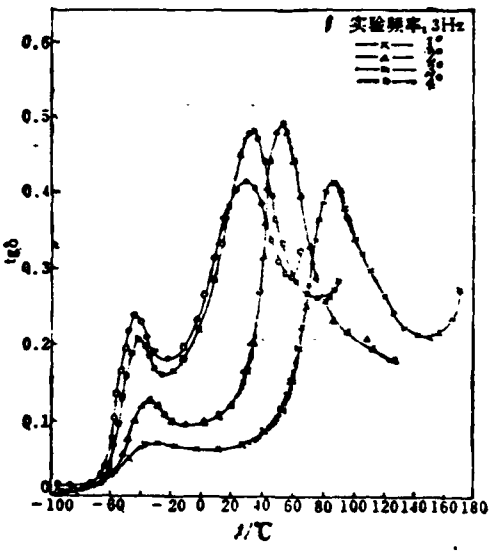

Fig. 3.8 tg_δ -t curves of samples 1*~4*.
1 - frequency

The ratio of NG to NC in samples 1*~4 change from 0.5 to 2. As shown in Fig. 3.8 Fig. 3.9, Fig. 3.10, the effect of NG on lowering the T_δ of the binder system is less than its effects on lowering the T_g of the same system (the main reason is the mobility of NG molecules getting smaller at low temperature). The effects of NG on the binder system are mainly shown in the main transition, but its plastification efficiency depends on the NG concentration. When the NG concentration reaches a certain amount, for sample 3* it was 58.51%, the decreasing of the T_g of the binder system slows down. The high elastic region is reduced and the viscous flow temperature T_f decrease is speeded up. This result coincides with usual effects of a plasticizer added to a rigid chain polymer.(12) Therefore, there is an optimal dose for NG to plasticize the binder system. With this dose the high elastic region

is widest.

To determine the best dose of NG, it can be started from cross linking NC. The sliding of molecule chains can be effeciently prevented. Thus, it is possible to continue increasing the dose of NG. This enables not only to decrease T_g, but also widen the high elastic region, and thus solve the problem caused by uncross-linked NC. Moreover, NG can also raise the low T mechanical damping. This is adventageous to raising the low T impact strengh of CMDB propellant. Therefore, cross-linking NC with prepolymerized additives enhances the flexible part at low temperature, coordinating with the adjustment of the NG dose. This is an effective way to improve the low T mechanical properties of CMDB propellant.

(3) The effects of different plasticizers

The experimental results of binder samples (12*, 13*, and 14*), which are made by adding different plasticizers (TA, DBP, and NG) into NC, are shown in Table 2.1 and Fig. 3.11. The results show that different plasticizers all cause β transition (this illustrates that this is due to β relaxation of the same mother structure of NC).

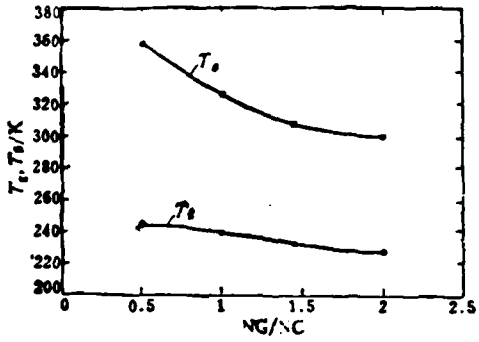

Figure 3.9. $T_\alpha(T_\beta)$-NG/NC curves of of samples 1*~4*.

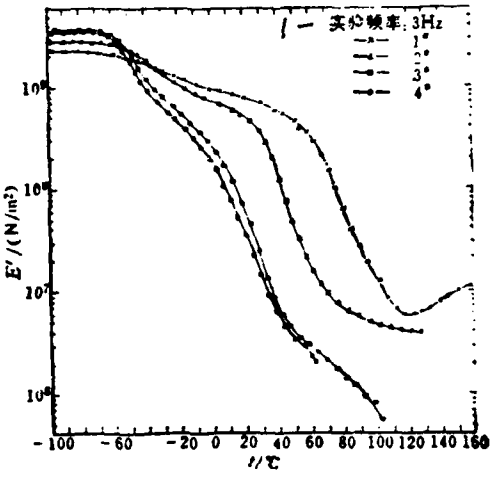

1-Frequency

Figure 3.10. E'-t curves of samples 1*~4*.

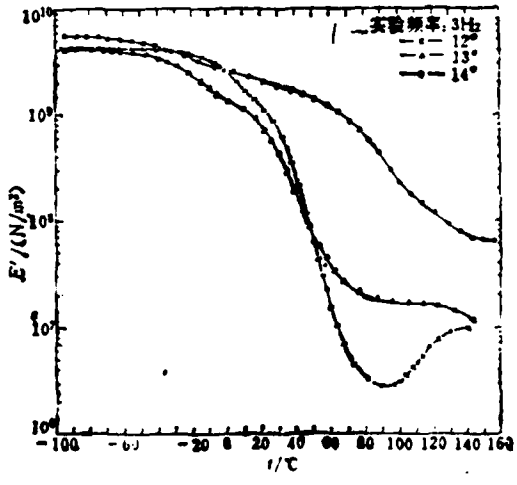

Figure 3.11. E'-t curves for samples 12*, 13* and 14*.

1. Frequency

But, with the same weight percentage concentration, the effects of NG on lowering the Tg and E' of NC is less notable than for TA or DBP. Therefore, under the prerequisite of not affecting the energy situation of CMDB propellants, using NG with other selected plasticizers will produce more efficient plastication.

(4) A trial quatitative analysis

According to the theory of isoviscosity state, one can treat the plasticizer and the polymer as polymer condensed solution system, and then use Flory's viscosity formula for condensed polymer solution to derive the qualitative relation between the polymer weight percentage W and the Tg of the condensed solution as follows:

$$\sqrt{W} = A' - \frac{E_v}{BRT_g}$$

where E_v-activation energy of viscous flow Tg-glass transition temperature (K) A' and B constants, assuming Ev independant of W. The double-base binder is NC condensed solution system according to the conditions described above. For the isoviscosity state at Tg, Ev approximates a constant, so (-Ev/Br) can be considered as a constant D. Hence,

$$\sqrt{W_{NC}} = A' + \frac{D}{T_g}$$

$\sqrt{W_{NC}}$ versus 1/Tg for samples 1*~4* are plotted in Fig. 3.12. Using linear regression one can obtain A'= 1.9625, D= -410.85, the linear correlation coefficient is -0.99504, showing a very good linear relation. So the empirical equation of the relation between $\sqrt{W_{NC}}$ and Tg for the double-base binder system, when NC weight percentage concentration is in 33.04-65.50% region, settling agent/NC = 0.0260, and under the 3 Hz dynamic condition, is

$$\sqrt{W_{NC}} = 1.96 - 4.11 \times 10^2 \frac{1}{T_g}$$

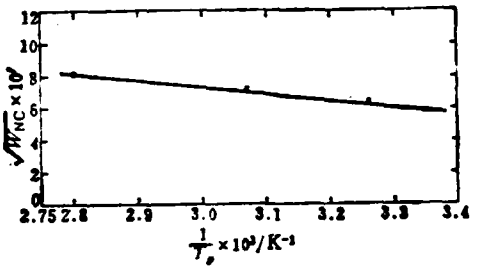

Fig. 3.12 The $\sqrt{WNC}$ -1/Tg relation of samples 1*~4*.

4. Conclusion

(1) The dynamic mechanical properties of CMDB propellant are between those of DB propellant and PVC composite propellant. In the usage temperature region, it passes through the glass phase region (has undergone relaxation), the glass transition region, and the high elastic region. Its transition region is very wide, so it has the property of high mechanical damping in the whole temperature range. This property is adventageous to withstand fairly large motion loads caused by transportation, ignition of the engine, launching, flying and so on.

(2) CMDB propellant has a fairly strong β relaxation at temperatures below Tg. This increases the impact strength in Tg-T_3 region, thus improves its low T anti-impact property, enlarges its usage temperature region at lcw T. This is advantageous to the firing impact load for low temperature-resistance.

(3) The dynamic mechanical properties of CMDB propellant mainly depend on its binder system. Adding solid fillers does not

effect its transition temperature (T_g, T_β) very much, but raises the energy storage modulus E' (particulary in the high elastic region), and lowers low T mechanical damping. Therefore, the deformation capability of CMDB propellant decreases and brings about an adverse effect on its low T mechanical properties.

(4) There is an optimal dose of the double-base binder. Using this dose, the plastication of NG is remarkable, and its low T mechanical damping is enhanced. Using this dose, the widest high elastic region is obtained.

Using the same weight percentage concentration, the effect of NG on decreasing the Tg and E' of NC is less than for TA and DBP.

(5) The 1/Tg of the double-base binder system has a linear relation to ½ the square of W_{NC}, which is the weight percentage of the nitrofibre.

(6) Using a viscoelastic meter to measure the dynamic mechanical properties of a solid propellant over a wide temperature and frequency range, the characteristic region of its viscoelastic behaviour can be observed. Information such as the molecular motion-dependent glass transition, second transition, mechanical damping, and the effective activation energy of the transition, can be obtained. This is important for the study of the relationship between the microstructure of a propellant and its macroproperties, which is based on molecular motion. Moreover, in the process of developing and selecting propellants which are suitable for large strategic missiles, it is absolutely necessary to evaluate the mechanical properties of solid propellants in all respects.

Acknowledgment

We borrowed some measuring equipment from the Chemistry Institute of the Chinese Academy of Sciences, and were helped by comrades Qi Zongneng and Zhan Wenzong.

〔1〕 Hufferd W. L. and Fitzgerald J. E., Development of a solid propellant viscoelastic dynamic model appendix a., N76-25433, (1976).
〔2〕 Kinloch A. J. and Gledhill R. A., Propellant failure, a fracture mechanich approach AIAA80-130, (1980).
〔3〕 Gordon S. and Darwe H. M., Composite modified cast-double-base propellants technology and application 9th International Aeronautical Congress, 1969.
〔4〕 Kaufman H. S. (ed), Introduction to polymer Science and techology, New York, Wiley-Interscience, 1977.
〔5〕 Nielsen L. E. 著，丁佳鼎译，《高分子和复合材料的力学性能》，北京，轻工业出版社，p. 230, 1981.
〔6〕 成都科学技术大学、天津轻工业学院、北京化工学院合编《高分子化学及物理学》，北京，轻工业出版社，p. 160-162, 1981.
〔7〕 Karger-Kocsis J. and Kuleznev V. N., *Polymer* Vol. 23, No. 5, 699-705(1982).
〔8〕 Nielsen L. E. 著，冯之榴等译，《高聚物的力学性能》，上海科学技术出版社，p. 198, 1965.
〔9〕 Nielsen L. E., *Appl polymer Symposia*, No. 12, 249-265, (1969).
〔10〕 Cantey D. E., Solid propellant structural integrity investigations, dynamic response and failure mechanisms, AD-452689, (1965).
〔11〕 Cantey D. E., Solid propellant structural integrity investigations, dynamic response and failure mechanisms, AD-610615, (1965).
〔12〕 金日光，高分子物理学基础理论讲座，《塑料》，(总31)，p. 79-80, 1979年增刊.
〔13〕 徐家麟，《化学通报》，北京，科学出版社，No. 5，1 (总257)(1965).

END

DTIC

8-86